Hg-DYNAMICS II

EXPERIMENTAL INVESTIGATIONS
ON THE FLOW OF MERCURY IN A HOMOGENEOUS
MAGNETIC FIELD

BY

JUL. HARTMANN AND FREIMUT LAZARUS

Introduction.

The main purpose of the investigations described in the present paper has been to study the influence of a homogeneous magnetic field on the flow of a conductive liquid — mercury — in pipes of circular or rectangular section. In a previous paper[1] this influence was examined theoretically on the assumption of a laminar flow in a flat channel of rectangular section, the field being perpendicular to the channel-sides of largest extension and the two other sides being formed by electrodes of highly conductive material. The experiments to be considered in the following were planned chiefly with a view to testing the main re- sults of the theoretical discussion. They have, however, in addition thrown light upon phenomena not readily open to such discussion, in particular upon the influence of a homogeneous magnetic field on a turbulent flow and the transition of the turbulent form of flow into the laminar. In this respect the present work may be regarded as an extension of an investigation performed several years ago in the same laboratory and having as subject the com- parison of the flow of water and mercury in pipes[2]. The

[1] Theory of the laminar Flow of an electrically conductive Liquid in a homogeneous magnetic Field. Det kgl. Danske Vidensk. Selsk. math.- fys. Medd. XV, 6, 1937.

[2] A Comparison between the Flow of Water and Mercury in Pipes etc. Mémoires de l'Académie Royale des Sciences de Danemark, Section des Sciences 8me Série, t. X, no 5. 1926.

1*

latter investigation showed that the REYNOLDS' Law of Similarity holds good for mercury even in cases in which the walls of the pipe are not wetted by this liquid. The investigations here reported amply confirm this fundamental experience.

I. The experimental Arrangements.

The general Arrangement.

In fig. 1 a diagram is given of the general experimental arrangement. A hydrodynamic circuit is used in which the flow is maintained by an electromagnetic pump $P.$[1] R is
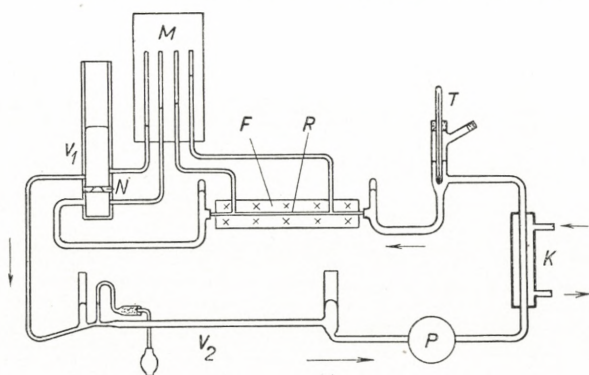

Fig. 1. General experimental Arrangement.

the duct — a glass tube or a rectangular channel in which the flow is examined. It is arranged in a homogeneous magnetic field F between the polepieces of a special electromagnet. The pressure drop in a certain length of the duct is observed by means of two manometer tubes connected to sockets on the duct. The volume of mercury passing each section of the circuit pr. sec. is measured by a simple flow meter of the calibrated nozzle pattern V_1. For rapid control of the volume flow a special flow meter V_2 was

---

[1] The principle of this pump is described in the paper referred to in note 1, p. 3.

furnished. As the mercury was heated by the current passed through the electromagnetic pump a cooling device K had to be introduced, the temperature being controlled by the thermometer T and kept at 20° C. A photograph showing part of the circuit and particularly the electro-
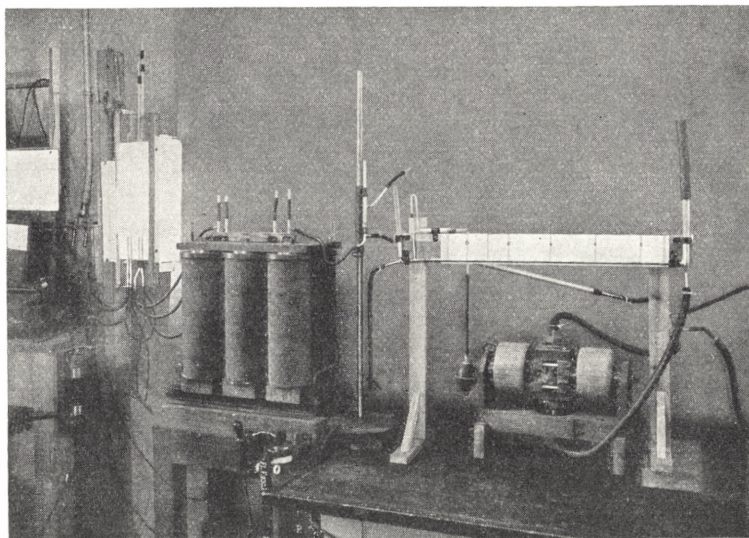

Fig. 2. Photograph of experimental Arrangement.

magnetic pump (to the right) and the electromagnet (to the left) is reproduced in fig. 2.

The various members of the experimental circuit will be described in detail below. Here some words may be said about the preparation of the ducts, especially the glass tubes. These were all comparatively narrow. Now, when a capillary has not undergone a special cleaning process the results of the flow experiments are quite indeterminate. This is due to a thin film of impurities adhering to the interior walls. In order to remove this film or layer the glass capillaries were for hours treated with concentrated

sulphuric acid with potassium bi-chromate $K_2 Cr_2 O_7$. Here-
after they were washed first with water and then with
absolute alcohol. If the capillaries were then dried by
drawing a flow of dry air through them the results of the
experiments were reproducible with an exactitude of a few
tenths of one p. c. and remained so for a very long time,
provided the capillaries were not emptied and the mercury
was thoroughly cleaned and dried before being introduced
into the circuit.

With the rectangular ducts the use of the cleaning
method here indicated was practially precluded. Instead
the walls were treated with benzol in a way described
below.

Measurement of the Flow of Mercury.

The flow of mercury, i. e. the volume V passing each
section of the circuit per. sec., was, as indicated, normally
measured by means of a nozzle N through which the flow
had to pass as indicated in fig. 1. The nozzle was arranged
in a vertical tube and could readily be interchanged. Seven
nozzles were used. In Tab. I the diameters of the bores
are stated in the first column.

Tab. I.

Constants of Nozzles used in Measurement of Flow.

Orifice mm.	Constant k
2.950	1.960
2.043	1.000
1.551	0.584
1.106	0.294
0.832	0.179
0.651	0.111
0.412	0.0463

In the second column the constant k of the apparatus defined by

(1) $$V = k\sqrt{h} \text{ cm.}^3/\text{sec.}$$

is entered. In the formula (1) h is the pressure drop in the nozzle measured in cm. Hg.

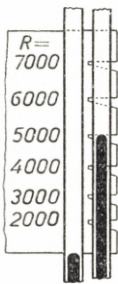For the observation of h the manometer tubes shown in fig. 1 were employed. The tubes were mounted on a transparent mm.-scale illuminated from behind. During each of the original experiments the magnetic field intensity H was kept constant and the flow adjusted for a series of values of the Reynolds' number R. With each experimental pipe or channel a set of experiments corresponding to a certain number of H-values was performed. In order to facilitate the work a card-board with notches as indicated in fig. 3 was produced corresponding to each experimental pipe or channel. When the pressure drop was equal to the distance from the lower edge of the card-board to the horizontal edge of a certain notch the Reynolds' number of the flow in the experimental duct had the value written sidewards to the notch in question. From this it will be gathered how the card-board was used for rapid setting of the flow during an experiment.

Fig. 3. Card-board with Notches for rapid Control of the Volume Flow.

It was found expedient to supplement the above described flow meter by another apparatus intended particularly for rapid control of the nozzle gauge. The apparatus referred to is indicated by V_2 in fig. 1. In fig. 4 it is shown on a larger scale. It consists mainly of a glass pipe *BCD* of known calibre. Just in front of the entrance to this pipe an air bubble may be pressed into the flow of mercury.

This bubble is carried with the flow and what is now measured is the time of its passage over the known distance between two marks C and D on the pipe. From this measurement and the calibre of the pipe the volume flow in the circuit is readily derived.

There are several precautions to be taken in the design and use of the flow gauge here considered. The bubble must fill out the whole section of the pipe. Therefore the
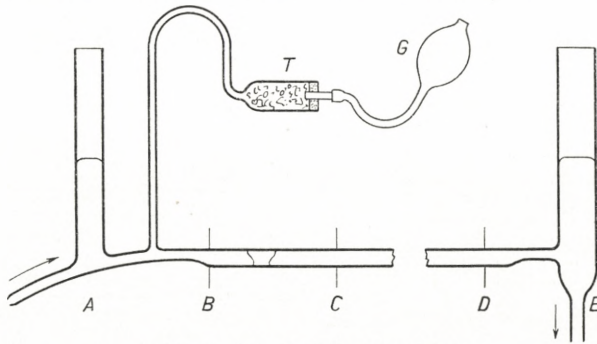

Fig. 4. Air Bubble Flow Meter.

aperture of the pipe must not be too large; in the apparatus in question it was 5.25 mm. At the moment at which the bubble is introduced slight fluctuations of the velocity will occur. So the bubble has to pass a certain length (9 cm.) of the pipe before entering the range CD which in the apparatus in question was 37 cm. It is absolutely essential that the walls of the pipe should be clean and dry; they were made so by the same method as was employed with the experimental capillaries. The air introduced into the pipe must also be dry and was therefore led through the tube T with a water absorbing material. In front of the inlet end of the apparatus a reservoir was arranged to stamp out the vibrations caused by the introduction of the bubble. At the exit end of the pipe another reservoir

was mounted, through which the bubble escaped after having passed the stretch *CD*.

The apparatus here described was, as stated, mainly used for quick control of the nozzle meter. In such a check the manometers of the latter gauge were always read during the passage of a bubble, because the bubble gave rise to a slight reduction of the velocity of the flow. The accuracy
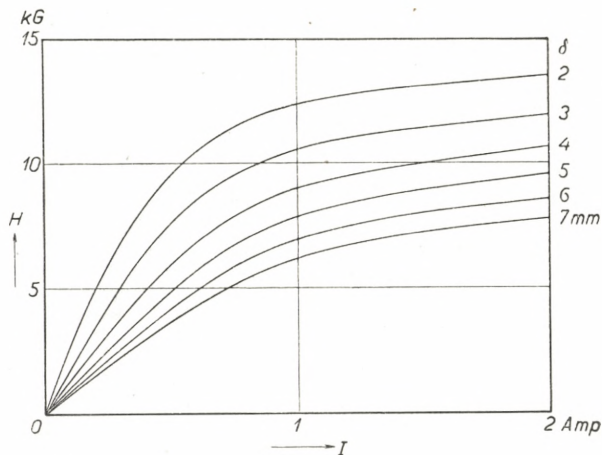

Fig. 5. Field-Intensity Curves at various Air Gaps.

of the measurement with the bubble apparatus was normally about 0.5 p. c.

The Magnet.

The construction of the magnet will appear from fig. 2. The length of the field was 36 cm., the height of it 1.67 cm. Field intensity curves (with the exciting current as abscissa) were plotted for the values 2, 3, 4, 5, 6, 7 mm. of the width δ of the air gap. These curves are reproduced in fig. 5. It should be noted that with the air gap 2 mm. and a field intensity $H = 8000$ Gauss the intensity at points 3 cm. from the ends of the pole-pieces was but 1.5 p. c. smaller

than at the middlepoint of the field. This lack of homo-
geneity was eventually reduced to 0.7 p. c. by an artificial
straying applied to the centre of the field. Everything goes
to show that this degree of homogeneity amply suffices
for the purpose in question. It is a well-known fact that
the field intensity is not a definite function of the exciting
current unless certain precautions are taken. In the case
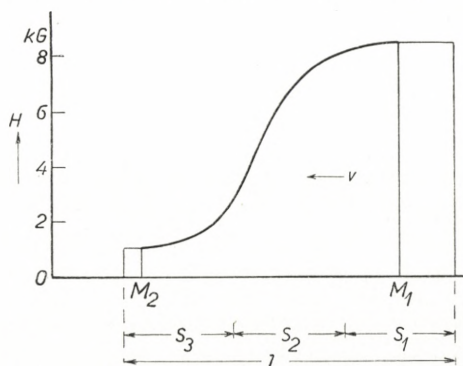considered a definite value of the field intensity was obtained

Fig. 6. Non-homogeneous magnetic Field produced by making one Set
of Magnet Coils currentless.

by approaching the value of the magnetising current through
a series of slow periodic current variations with an am-
plitude gradually going down to zero. This method was also
used for demagnetising the magnet when the pressure drop
was to be read corresponding to zero field intensity.

In connection with the magnet some observations on the
effect of a non-homogeneous field on the pressure drop in the
flow should be mentioned. Of the three sets of magnet coils
(fig. 2) the set next to the exit end of the experimental duct
was made currentless. In this way a field distribution curve like
that indicated in fig. 6, where M_1 and M_2 are the positions of the
manometer sockets, was obtained. The direction of the flow in
the duct is indicated by the arrow. The flow thus first passes
the stronger part of the field before entering the more feeble part.

With a volume velocity or, which is the same, a Reynold's number R well within the domain of laminar flow the observed pressure drop was not that corresponding to a homogeneous field of an intensity equal to the average value of the field — the average intensity was 4800 Gauss — but that corresponding to the higher field intensity 5200 Gauss. (Compare curves 9—18 below). On the other hand, if the set of coils at the inlet end was made current-less so that the flow took place in the direction from a lower field intensity to a higher one the observed pressure drop corresponded to a lower field-intensity — 5700 Gauss — than the average — 5900 Gauss. These observations find their explanation in the well-known fact that it takes time to change the velocity distribution — on which the pressure drop depends. The distribution corresponding to the field at the inlet end of the duct persists in some degree after the flow has left this field.

It was concluded from the experiments here indicated that the additional pressure drop to which the non-homogeneity illustrated in fig. 6 gave rise was otherwise practically imperceptible — in spite of the extremely pronounced character of the non-homogeneity. Thus homogeneity is required less in order to avoid this additional pressure drop than on account of the source of error illustrated by the experiments referred to above.

The experimental Tubes and Channels.

Five cylindrical glass tubes, indicated in Tab. II below by the numbers 11—15, were used in the experiments here considered. They were selected from a large stock and were carefully calibrated. In no tube did the diameter vary more than about 0.5 p. c. within the part in which the pressure drop was measured. This part has a length of 28 cm. It was of course arranged entirely within the magnetic field. The whole length of the tube was 43 cm. the extensions on either side of the stretch of observation being 7.5 cm. At the inlet end of the tube 6 cm. of the 7.5 cm. were inside the magnetic field, at the exit end 2 cm. As stated elsewhere, the edge of the experimental tube or pipe was

kept sharp in order to secure transition from laminar to turbulent flow at a definite value of the velocity or of the Reynolds' number. The thickness of the wall of the tube was taken as small as possible, about 0.8 mm., with a view to reducing the air gap of the magnet, and so to be able to produce magnetic fields of the greatest possible intensity.
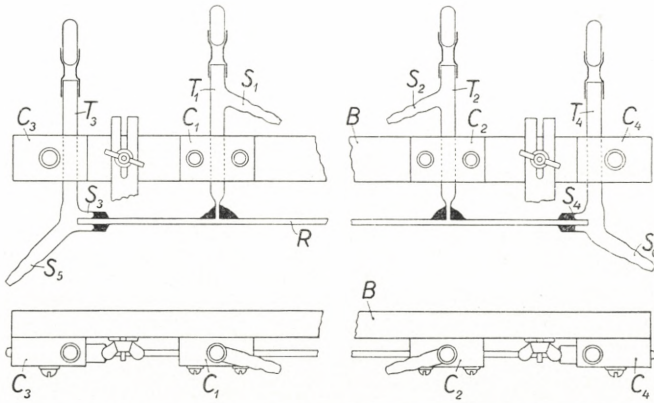
Connections to the manometer tubes were obtained

Fig. 7 a. Mounting of a cylindrical experimental Glass Pipe.

through bores at either end of the 28 cm. stretch of observation. The production of the bores by means of a swiftly rotating copper plug covered at the flat end with oil and carborundum required some practice. Slight annealing of the tube by drawing it through a luminous gas flame would seem a wise precaution before the process of boring in order to render breaking of the tube less likely.

The way in which the tube is mounted will appear from fig. 7 a. B is a light bar of wood to which four wooden blocks are fastened. The two extreme blocks $C_3 C_4$ carry two glass tubes or "shafts" $T_3 T_4$, each with a rather wide socket, $S_3 S_4$. Into these sockets the ends of the experimental

tube R are "cemented" by means of "picein". Above the bores in the experimental tube are placed two shafts T_1 and T_2, carried by the blocks C_1C_2 and cemented to the experimental tube likewise by picein. On T_1 and T_2 are the two sockets S_1S_2 for the rubber tubes to the manometer. The flow of mercury is passed into and out of the experimental pipe by the sockets S_5S_6. The shafts $T_1T_2T_3T_4$ serve as traps for dust particles and minute air
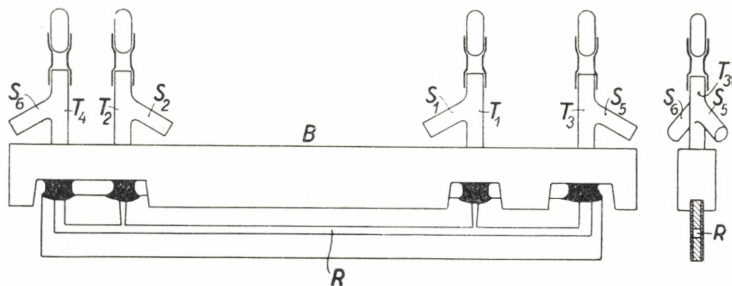

Fig. 7 b. Mounting of rectangular Channel.

bubbles. They are closed above by stoppers made from glass tubes.

We pass on to the rectangular ducts. Of these 18 were produced. They are indicated as $K\ 21$—$K\ 38$ in Tab. II. In $K\ 21$ the distance between the manometer sockets was 28 cm., in all the other ducts 14 cm. The total length of the ducts was in the latter cases 20 cm., the whole duct being mounted within the magnetic field. Fig. 7 b illustrates the mounting of a duct. The figure will be understood from the explanation given in connection with fig. 7 a. It may just be noted that the distance between T_1 and T_3 was 4 cm., that between T_2 and T_4 2 cm., finally that the flow was in the direction from T_1 to T_2.

In fig. 8 a section of a duct is shown. The rectangular channel is formed between the plates BB and the pieces

Tab. II.

List of experimental Ducts.

No.	r cm.	L cm.	$\nu_T \cdot 10^5$ at 20° C.	$\nu_L \cdot 10^5$ at 20° C.
11	0.0345	28.02	113	115
12	0.0583	27.93	121	121
13	0.0923	28.00	114	127
14	0.1147	28.02	123	—
15	0.1647	28.00	117	—

No.	a cm.	b cm.	$\dfrac{a}{b}$	$\nu_L \cdot 10^5$ at 20° C.
K 21	0.030	0.186	0.161	137
K 22	0.014	0.0625	0.224	99
K 23	0.0145	0.254	0.057	112
K 24	0.090	0.060	1.50	—
K 25	0.090	0.035	2.57	130
K 26	0.091	0.1075	0.846	167
K 27	0.091	0.081	1.12	170
K 28	0.091	0.0915	0.995	164
K 29	0.154	0.0415	3.71	145
K 30	0.155	0.060	2.58	159
K 31	0.155	0.1345	1.15	250
K 32	0.056	0.0935	0.60	130
K 33	0.057	0.058	0.99	130
K 34 ⎫ Cu	0.155	0.030	5.16	178
K 35 ⎭	0.155	0.0525	2.95	75
K 36	0.157	0.0338	4.65	95
K 37	0.157	0.042	3.75	135
K 38	0.157	0.055	2.88	158

AA. With the ducts K 34 and K 35, AA were made of copper, the surfaces forming the top and the floor of the channel being in these cases amalgamated. These ducts were made to agree exactly with the duct for which the theory was developed. With the other ducts AA were made of wood or "fiber". In the ducts K 21 to 28 BB were made
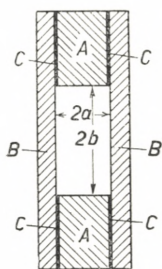
Fig. 8. Cross-section of experimental Channel.

of glass, in the others of celluloid. C is the cement between A and B; generally "asphalt lac" was employed. After the cementing together of the pieces A and B, lac would as a rule have entered the duct and had to be carefully removed by means of small pieces of cotton, wetted with benzol, which were pushed or drawn through the duct. The dimension $2b$ was measured by means of a microscope, while $2a$ was calculated from the total thickness of the duct and from the thicknesses of the B-sheets.

II. The Results and their Discussion.

Review of the Results.

For each tube or channel the variation with the magnetic field intensity of the pressure drop between the two sockets was determined for a number of values of the volume velocity V or of the Reynolds' number R. The latter is, in the case of a cylindrical pipe, defined by

$$(1) \qquad R = \frac{v \cdot r}{\nu} = \frac{V}{\pi r \nu}$$

where v is the average velocity in cm./sec. over the section of the pipe, r the radius of the circular section in cm. and $\nu = \frac{\eta}{\varrho}$ the dynamical viscosity, i. e. the ratio of the viscosity and the density in c. g. s. units. In the case of a rectangular section, $2a \cdot 2b$, r means the hydraulic radius defined as

$$(2) \qquad r = \frac{2F}{O} = \frac{2ab}{a+b}$$

where F is the area and O the circumference of the cross-section.

The results of the experiments with each pipe or channel were represented in the shape of a series of curves having as abscissae the intensity H of the magnetic field, as ordinates the pressure drop h between the sockets measured in cm. Hg. Complete, representative sets of experiments are given in figs. 9—18. In each figure the dimensions of the pipe or channel are stated together with the length l (L in Tab. II) in which the pressure drop was measured.

It is well known that the turbulent flow in a pipe is changed into a laminar flow if the velocity or the REYNOLDS' number is reduced below a certain value. This value may be taken to be $R = 1160$ (c. g. s.). A laminar flow may, on the other hand, be maintained even if the REYNOLDS' number is raised considerably above the critical value, provided the inlet end of the pipe is smooth and all disturbances of the flow are otherwise avoided. In the experiments here considered the edges of the pipe or channel were deliberately kept sharp in order to secure in every case a well defined transition from a laminar to a turbulent flow.

In the diagrams reproduced in figs. 9—18 this transition is clearly seen in all cases where a turbulent flow is observed. A curve is drawn through all the points of transition. Above and to the left of this curve, which is of a parabolic character, we have the domain of turbulent flow, below and to the right that of laminar flow. Within the first region the pressure drop and so the apparent viscosity decreases with increasing intensity of the magnetic field. This is due to the damping effect of the field on the vortices in the flow. Within the domain of laminar
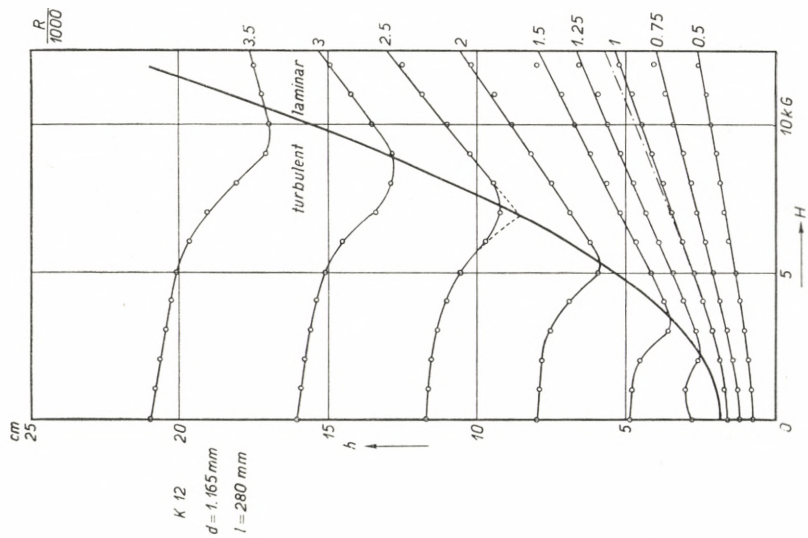
Fig. 10.

Fig. 9.

Fig. 12.

K 21

$2a = 0.60$ mm
$b = 3.72$ mm
$l = 280$ mm

Fig. 11.

K 23

$2a = 0.291$ mm
$2b = 5.08$ mm
$l = 14.0$ mm

2*

Fig. 14.

Fig. 13.

Fig. 16.

K 27

$2a = 1.82\,mm$
$2b = 1.62\,mm$
$l = 140\,mm$

Fig. 15.

K 33

$2a = 1.15\,mm$
$2b = 1.16\,mm$
$l = 140\,mm$
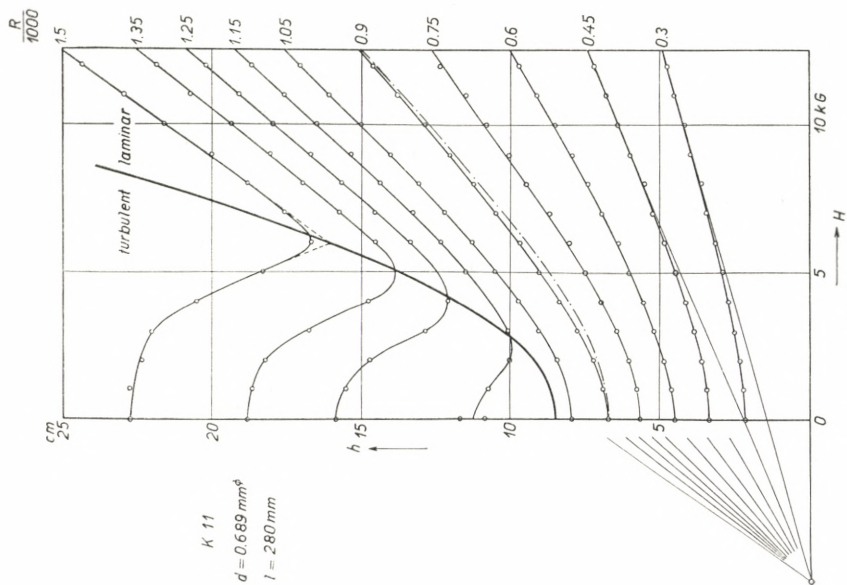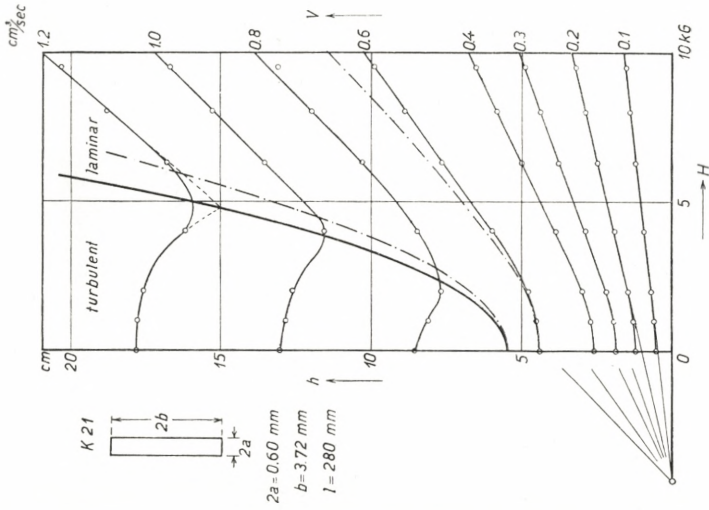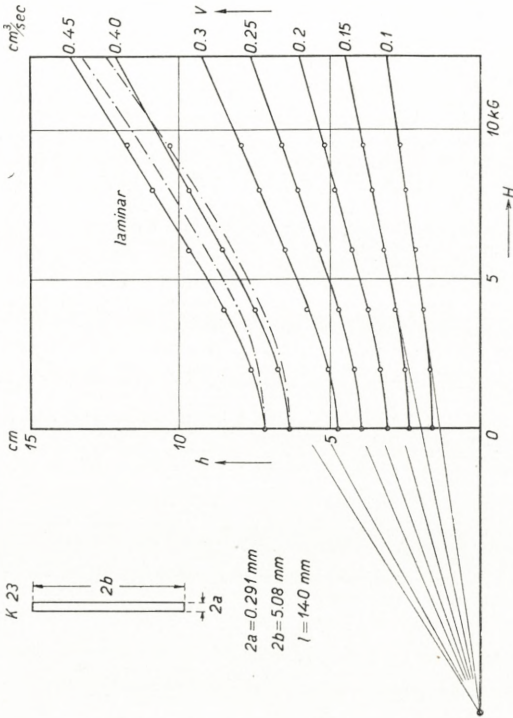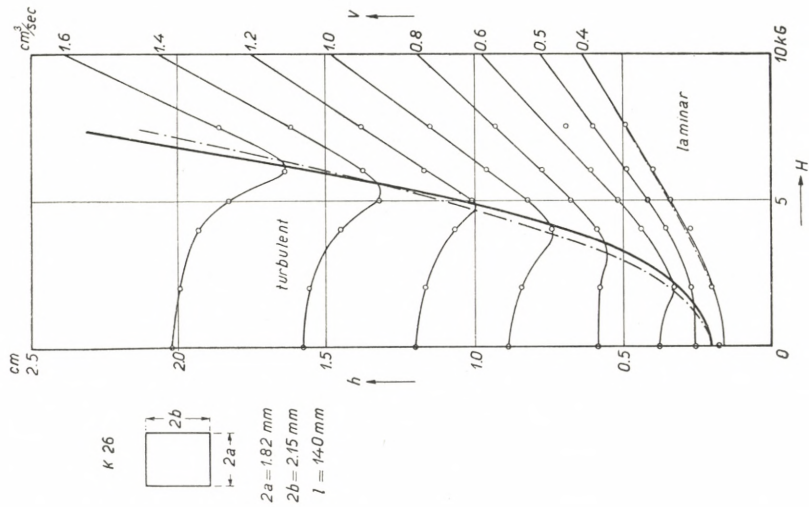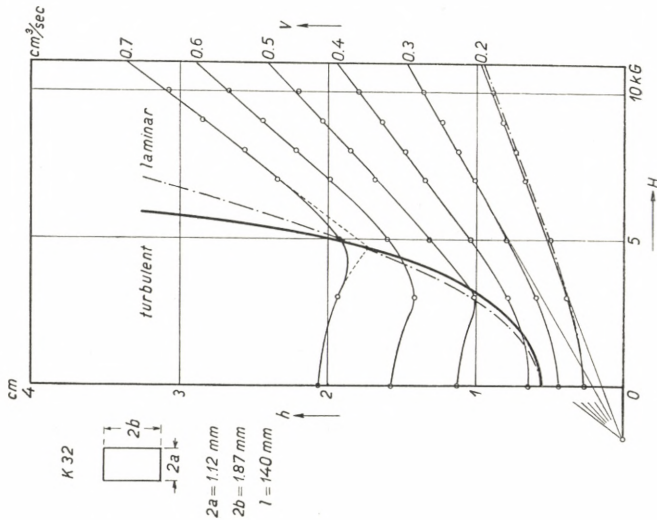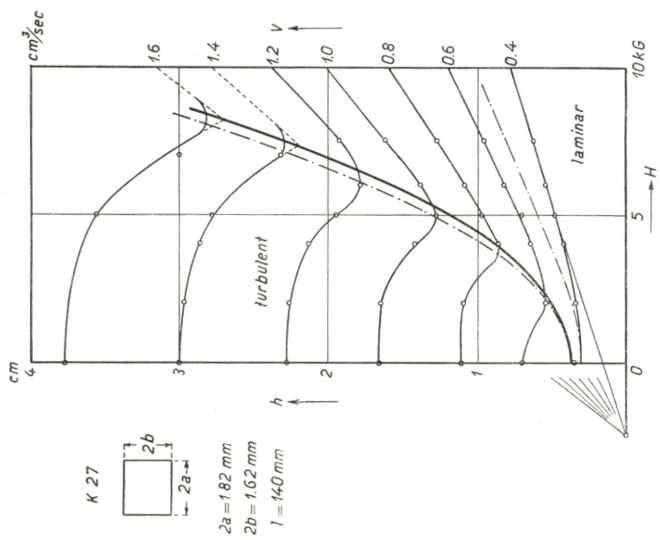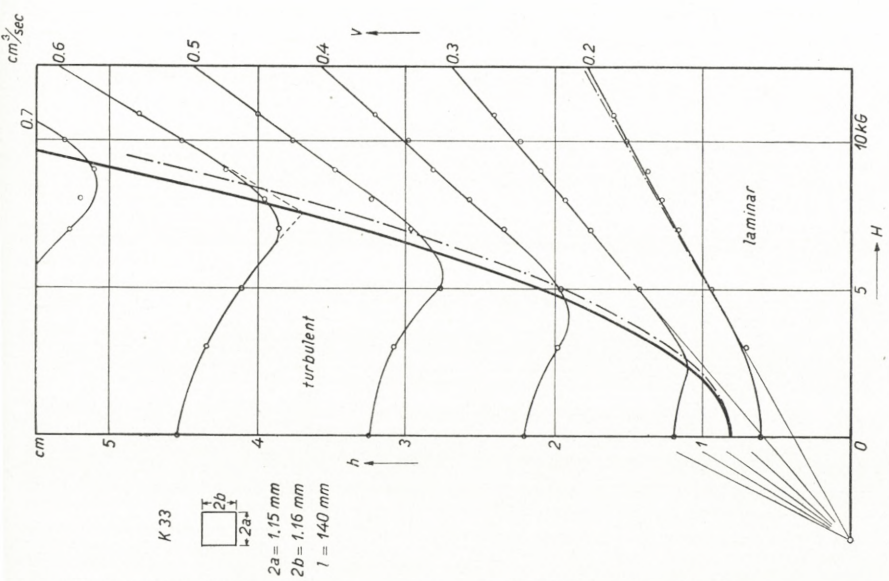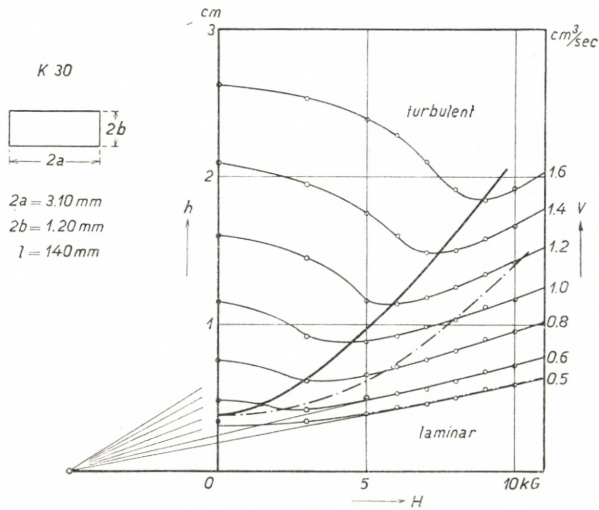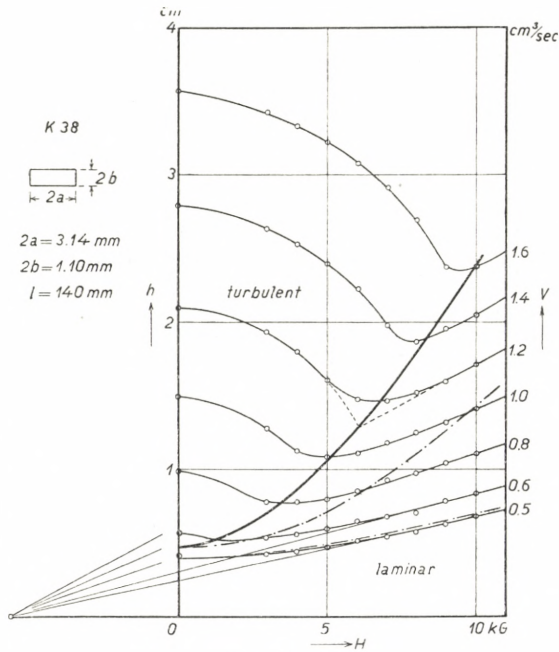
Fig. 17.

Fig. 18.

Fig. 9—18. Variation of Pressure Drop with Intensity of the magnetic Field.

flow the pressure drop increases rapidly with the field intensity. In cases where the flow is still laminar with no magnetic field on, the pressure drop may readily be raised to values twice the value corresponding to $H = 0$ by putting on a field of quite moderate intensity. As a matter of fact the curves indicate that the pressure drop may be raised to any value by increasing the field since obviously the drop increases approximately as the field intensity when this is not too small. That is to say: the effect of the field on the laminar flow is to increase the apparent viscosity approximately proportionally to the field intensity. With rather small values of the field the apparent viscosity varies within the domain of laminar flow in a parabolic manner. The facts here stated may now be compared with the predictions of the theory referred to in the introduction to the paper. — It should, however, be borne in mind that the theory is based on certain simplifying assumptions and can only be expected to hold good in cases where these assumptions are fulfilled.

Comparison with the Theory.

The main predictions of the theory may be thus stated.

In a narrow channel of rectangular section $2a \cdot 2b$ cm.[2] ($b >> a$) placed in a homogeneous magnetic field of intensity H Gauss perpendicular to the side of the largest extension ($2b$) there will, when the channel is passed by a laminar flow $V \frac{\text{cm.}^3}{\text{sec.}}$ of an electrically conductive liquid, be a pressure drop p dyne/cm. determined by the formula:

(1)
$$p = \frac{3\,VL}{4\,ba^3}\eta_e' \quad \frac{\text{dyne}}{\text{cm.}}$$

where

(2) $$\eta'_e = \frac{\eta}{3} \cdot \frac{z_0^2 \tanh z_0}{z_0 - \tanh z_0} = \frac{\eta}{3} f(z_0)$$

where, again,

(3) $$z_0^2 = 10^{-9} \frac{H^2 a^2}{\eta \varkappa}.$$

Here L is the length of that part of the channel in which the pressure drop is measured, $\varkappa$ the specific resistivity of the liquid while η'_e is the apparent or virtual viscosity óf the liquid in the magnetic field under the prevailing conditions. If z_0 is small compared to 1 the apparent viscosity η'_e may be expressed by

(2a) $$\eta'_e = \eta + \eta_e = \eta + \frac{1}{15} 10^{-9} \frac{H^2 a^2}{\varkappa}$$

showing that η'_e and so the pressure drop is that corresponding to zero field increased by an amount, the electro-magnetic viscosity resp. the electro-magnetic pressure drop, which increases proportionally to the square of the field intensity. If z_0 is large compared to 1 (strong fields) we derive the expression:

(2b) $$\eta'_e = \frac{1}{3} \sqrt{10^{-9}} \, Ha \cdot \sqrt{\frac{\eta}{\varkappa} + \frac{\eta}{3}}$$

from which it is seen that the apparent viscosity η'_e and so the pressure drop now increases linearly with H. The description of the conditions with a laminar flow in a homogeneous magnetic field thus given by the theory obviously fits in qualitatively with the observations. Quantitatively the agreement can only be expected to be tolerably close with flat channels, i. e. with small values of a. Fig. 11 corresponds to such a channel, and just in this case a comparatively very close agreement was found, as will be seen from the direct comparison between the ob-

served and the theoretical curve made with the curve $V =$ 0.4 cm³./sec. It should be noted that the channel considered was not closed above and below by walls of highly conductive material as assumed in the theory. This, however, is obviously of small importance if only the channel is very high compared to its width, seeing that in this case the electric current lines remain practically rectilinear over most of the height of the section, while the conductive walls are replaced by the layers of mercury close to the top and the bottom of the channel.

Now the experiments not only cover cases in which the assumptions of the theory are fairly well fulfilled but also such in which the duct differs very much from a flat channel placed with its largest side perpendicular to the magnetic field. They even comprise investigations on the flow in cylindrical pipes. Obviously in such cases the theory as given by the equations (1)—(3) cannot be expected to hold good directly. It must be modified in some way or other and it is with this modification or adjustment we are concerned in the following. We may divide our problem into two. The pressure drop in cm. *Hg*, the quality directly observed, may according to (1) and (2) be written

(4)
$$h = \frac{3\,VL\,\eta}{4\,ba^3\varrho\,g} \cdot \frac{f(z_0)}{3}\ \text{cm. } Hg.$$

The coefficient to $\dfrac{f(z_0)}{3}$ is simply the expression for the pressure drop h_0 in a narrow channel when not placed in a magnetic field. If the channel is not narrow or if the duct is a cylindrical pipe the coefficient to $\dfrac{f(z_0)}{3}$ in (4) should obviously be replaced by an appropriate expression corresponding to the duct in question. The function $\dfrac{f(z_0)}{3}$ ex-

presses the change of the pressure drop to which the
magnetic field gives rise (in the case of a laminar flow).
In accordance herewith it is 1 for $H = 0$. It will be noted
that the general character of the h-H-curves is in all cases
much the same. This suggests that the function $\dfrac{f(z_0)}{3}$, devel-
oped for the special case of a flat channel, may be made
to cover other cases by applying a suitable reduction factor
to the variable z_0 or H.

The points of view here set forth are tested in the
following paragraphs.

The Flow at Zero Field-Intensity.

The expression to replace the coefficient to $\dfrac{f(z_0)}{3}$ in
equation (4) of the preceding paragraph is with a cylindrical
pipe of radius r

(1)
$$h_0 = \frac{8}{\pi} \cdot \frac{LV\nu}{r^4 g} = \frac{8L\nu^2}{r^3 g} \cdot R,$$

ν being the dynamical viscosity and R being the Reynolds'
number defined by

(2)
$$R = \frac{v \cdot r}{\nu}.$$

With channels of rectangular section — sides $2a$ and $2b$
— a method for the calculation of the pressure drop at
zero field-intensity is arrived at in the following way.

The Poiseuille Law for the laminar flow in a cylindri-
cal pipe, i. e. (1), may be written in the form

(3)
$$\frac{2hrg}{Lv^2} \cdot \frac{v \cdot r}{\nu} = \psi \cdot R = 16,$$

where both ψ and R are dimensionless qualities. In case
of a pipe of rectangular section $2a \cdot 2b$ one may use the
same form for the law, writing

(4) $\psi R = K$

and replacing r by the "hydraulic radius" defined as the ratio of 2 times area of section and circumference. K, then, is a function of the ratio $\dfrac{a}{b}$ and for this function LEA and TADROS have given a curve reproduced in fig. 19[1]. In case
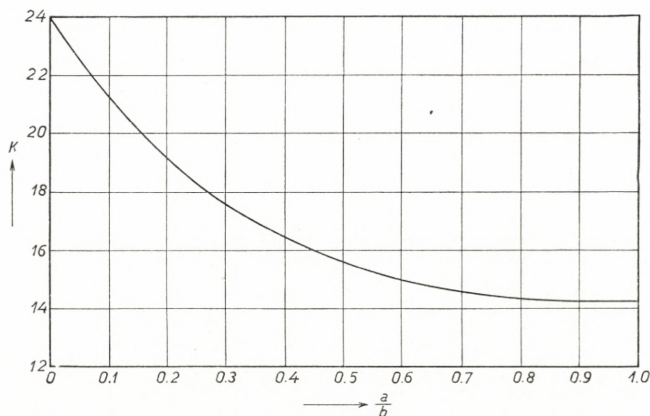
Fig. 19. Variation of $K = \psi R$ with $\dfrac{a}{b}$ for rectangular Pipes.
(LEA and TADROS).

of a very flat channel i. e. with $b = \infty$ the hydraulic radius is $2\,a$ and the formula (4) together with the value $K = 24$ taken from fig. 19 leads to the formula

(5) $h = \dfrac{3}{4} \dfrac{L\,\nu}{ba^3 g} \cdot V$ (Flat channel, $a << b$),

which may be directly derived. With a channel of quadratic section, $a = b$, the hydraulic radius is just equal to a. In this case the curve fig. 19 gives $K = 14.22$ and (4) may be written

[1] F. C. LEA and A. G. TADROS. Phil. Mag. (7), 11, 1235, 1931.

(6) $h = 1.78 \cdot \dfrac{L\,\nu}{a^4 g} \cdot V$ (Quadratic channel, $a = b$),

an expression which is a consequence of a more general for-
mula derived by Boussinesq and confirmed experimentally by
Schiller[1]. In the general case, the formula for the pressure
drop becomes:

(7) $h = \dfrac{K}{32} \cdot \dfrac{L\,\nu}{g} \cdot \dfrac{(a+b)^2}{a^3 b^3} \cdot V.$

Now plotting the pressure drops, observed for $H = 0$
within the domain of laminar flow, figs. 9—18, against R
or V, straight lines are found from the slope of which the
dynamical viscosity ν may be calculated on the basis of
expressions (1) and (7). In Tab. II the values thus deter-
mined are stated under ν_L. With cylindrical pipes values
are found of much the same size, viz. $117 \cdot 10^{-5}$, the value
which is generally accepted for mercury at $20°$ C. With
the rectangular ducts the results are rather fluctuating.
This is thought to be due to difficulties in the production
of the ducts and in the cleaning of them.

Values for ν may also be calculated from the observ-
ations of the pressure drop in cylindrical pipes, at $H = 0$,
within the domain of turbulent flow, seeing that an em-
pirical formula has been derived by Blasius for this
domain. The formula is

(8) $h = 0.06652 \; v^{7/4} \cdot r^{-5/4} \cdot \nu^{-1/4} \cdot g^{-1}.$

By means of (8) the values of ν entered in Tab. II under
ν_T were found. As will be seen, they agree well with the
corresponding values from the laminar domain.

Fig. 20 illustrates the variation of the pressure drop h

[1] Comp. Handbuch der Experimentalphysik IV. 4 Teil 1932, p. 146.

with the REYNOLDS' number R. The curves are derived from
the diagram in fig. 9 corresponding to a cylindrical pipe.
It will be seen that h is, within the laminar domain, ex-

Fig. 20. Variation of Pressure Drop with REYNOLDS' Number R.
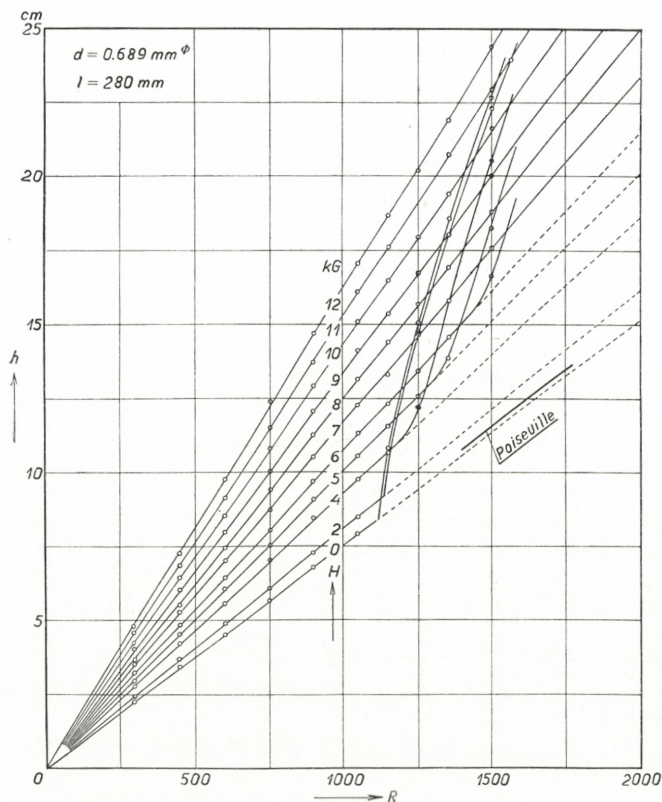
actly proportional to R as predicted by POISEUILLE's ex-
pression (1) for $H = 0$.

It is, however, not only so for $H = 0$ but for all values
of H. In the diagram, fig. 20, the variation of h with R
is also given for the turbulent flow. The transition, with
$H = 0$, takes place at $R = 1120$, i. e. not too far from the
generally accepted value $R = 1160$.

Adjustment of the Function $f(z_0)$ to fit the Observations.

The theory of the pressure drop with a flat channel can now be given in the general form

(1)
$$h = h_0(V) \cdot \frac{f(z_0)}{3}$$

where $h_0(V)$ is the pressure drop corresponding to zero field-intensity. The latter is proportional to the volume flow (or to the Reynolds' number).

We shall make an attempt at adjusting this theory for other ducts than a flat rectangular channel. In so doing we shall first try whether the pressure drop cannot be represented by the formula

(2)
$$h = h_0(V) \cdot \frac{f(c_1 z_0)}{3}$$

where c_1 is a number depending, with rectangular channels, on the value of $\frac{a}{b}$ only.

The way in which this attempt was performed may be thus explained. We start with a set of observed curves of the type of figs. 9—18, fig. 21 a. From this set we may derive another set, fig. 21 b, of the type of fig. 20. By means of the latter diagram we may construct the h-H-curve corresponding to $h_0(V) = 3$. The way it is done will be understood from the figure. The curve found in this way is $h = f(c_1 z_0)$ with H as abscissa instead of z_0. Now $z_0{}^2 = 10^{-9} \frac{H^2 a^2}{\eta \varkappa}$ from which with $\eta = 0.0159$ c. g. s. and $\varkappa = 10^{-4}$ Ohm·cm. (20° C.) we derive $z_0 = 0.0250 \, aH$. By means of the latter formula we transform the h-H-curve into the h-z_0-curve and thus have the curve which we try to express by $h = f(c_1 z_0)$. It is shown in fig. 21 c. In the same

figure the theoretical curve $h = f(z_0)$ is drawn. For a number of values of h the ratio of the corresponding ab-
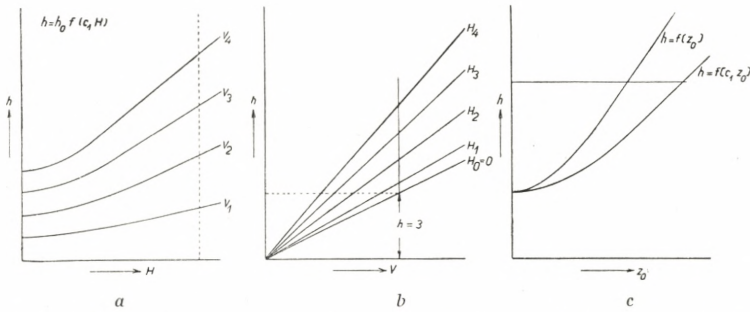
Figs. 21 a—c. Diagrams to explain the Adjustment of the Theory to fit the Observations.

scissae of $h = f(z_0)$ and $h = f(c_1 z_0)$ is calculated. This ratio c_1 is found to be tolerably constant independent of
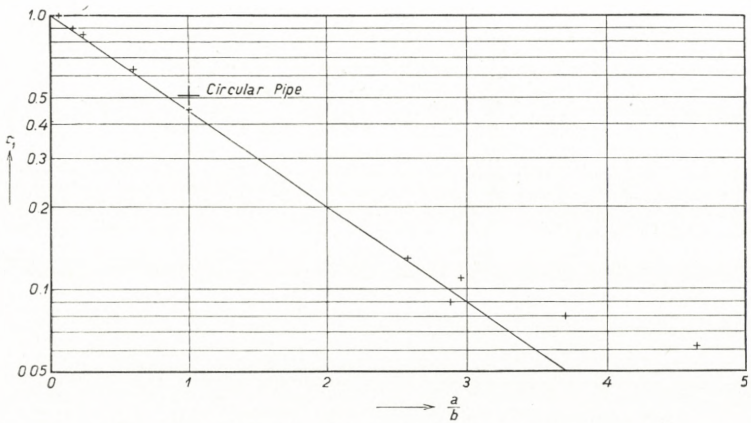

Fig. 22. Variation of the Reduction Factor c_1 with $\dfrac{a}{b}$.

h or z_0. So by multiplying the abscissae of the "observed" h-z_0-curve by a constant factor the curve is reduced to that corresponding to a flat channel (of which $c_1 = 1$). Or we may, in general, express the pressure drop in a

rectangular channel placed in a homogeneous magnetic field by the formula (2).

The value of c_1 of course depends on the ratio $\frac{a}{b}$ of the two sides of the channel cross-section (a parallel to the magnetic force). In fig. 22 the variation of c_1 with $\frac{a}{b}$ is shown. Up to $\frac{a}{b} = 3$ the variation may, in the semi-logarithmic system of coordinates, be represented by a straight line corresponding to the dependency

$$(3) \qquad c_1 = 10^{-0.35\,\frac{a}{b}}.$$

So, finally, the formula for the pressure drop in a rectangular channel may, with a laminar flow, be written

$$(4) \qquad h = h_0 \cdot \frac{f\left(z_0 \cdot 10^{-0.35\,\frac{a}{b}}\right)}{3} \text{ cm. } Hg, \ \frac{a}{b} < 3,$$

where the f-function is defined by

$$(5) \qquad f(x) = x^2\, \frac{\dfrac{\tanh x}{x}}{1 - \dfrac{\tanh x}{x}}.$$

With cylindrical pipes also the pressure drop with a laminar flow may be expressed by formula (2). The value which must here be ascribed to c_1 was found to be 0.51 independently of the radius r of the pipe, at any rate between $r = 0.35$ mm. and 0.92 mm. Thus with cylindrical pipes the pressure drop with a laminar flow is determined by

$$(6) \qquad h = h_0 \cdot \frac{f(0.51\,z_0)}{3} \text{ cm. } Hg,$$

where it should be noted that z_0 is calculated from the field-intensity H by the expression

(7) $$z_0 = 0.0250\, rH$$

r being the radius of the cross-section of the pipe.

In order to illustrate the agreement between the h-H-curves calculated by means of expressions (4) and (6) and the corresponding observed curves a calculated curve, the dot and dash curve, is plotted in each of the diagrams figs. 9—18[1]. It will be seen that in most cases the agreement is fairly good. It should be noted that the calculated curve is drawn with the same h_0 as the observed curve. No account has thus been taken of a possible error in the value of h_0.

In connection with the discussion here given attention may be called to a particular feature of the experimental curves of figs. 9—18. If, as indicated in the diagrams, tangents are drawn to the several curves of each set corresponding to the same abscissa (in the diagrams $H = 8000$ Gauss) it is found that all the tangents intersect in the same point of the axis of abscissae or nearly so. This feature is a direct consequence of the theory, whether in the original or in the modified form. For the theory may be written

(8) $$h = CV f(c_1 z_0), \quad z_0 = 0.0250\, aH.$$

From this expression it follows that

(9) $$\frac{dh}{dH} = \frac{dh}{dz_0} \cdot \frac{dz_0}{dH} = CV \cdot c_1 \cdot 0.0250\, a\, f'(c_1 z_0) = C_1 V.$$

The equation of the tangent to one of the H-h-curves at the point $(H_1,\, h_1)$ is

(10) $$\frac{h - h_1}{H - H_1} = C_1 V.$$

---

[1] In fig. 11 the test is made with $V = 0.45$ cm.^{3}/sec.

Hence the abscissa of the point of intersection with the axis of abscissae is determined by

(11) $H' = H_1 - \dfrac{h_1}{C_1 V} = H_1 - \dfrac{1}{0.0250\, ac_1} \dfrac{f(c_1 z_0)}{f'(c_1 z_0)}$

i. e. H' is independent of V. From the formula $f(z_0) = \dfrac{z_0^2 \tanh z_0}{z_0 - \tanh z_0}$ the following expression for $f'(z_0)$ may readily be derived:

(12) $f'(z_0) = \dfrac{z_0^3 \operatorname{sech}^2 z_0 + z_0^2 \tanh z_0 - 2\, z_0 \tanh^2 z_0}{(z_0 - \tanh z_0)^2}.$

By means of (11), (12) and the expression for $f(z_0)$ the experimental values found for H' could be checked. A test of this description would, however, seem superfluous after the discussion given in the first part of the present paragraph.

The Boundary Curve between the Domains of laminar and turbulent Flow.

In the experiments considered measures were taken to secure transition from a laminar to a turbulent flow at a definite value of the Reynolds' number R. The critical value may be denoted by R_c. It is determined by

(1) $$R_c = \frac{v_c \cdot r_h}{\nu}.$$

Here r_h is the hydraulic radius which with a channel of rectangular section $2a \cdot 2b$ is equal to $\dfrac{2\,ab}{a+b}$. Again v_c, the critical velocity, is equal to the volume-velocity V_c divided by $4\,ab$. Introducing in (1) this formula may be written

(2) $$R_c = \frac{V_c}{2\,(a+b)\,\nu} = \frac{V_c \cdot \varrho}{2\,(a+b)\,\eta}.$$

Now, if the flow takes place in a homogeneous magnetic field the transition is displaced towards larger values of the volume flow i. e. V_c increases. The explanation is most likely to be found in the apparent increase of the viscosity η. On this assumption the variation of the critical volume-velocity V_c with H should be

(3) $$V_c = \frac{2\,(a+b)}{\varrho}\,R_c \cdot \eta'_e = \frac{2}{3}\,\frac{a+b}{\varrho}\,R_c\,\eta\,f(z_0).$$

The corresponding value of the pressure drop h_c in the channel is determined by

(4) $$h_c = \frac{3}{4} \cdot \frac{V_c L}{b a^3}\,\eta'_e = \frac{1}{6}\,R_c\,\frac{a+b}{b a^3} \cdot \frac{L}{G} \cdot \nu^2 f^2\,(z_0).$$

Instead of the critical REYNOLDS' number we may here introduce the critical volume-velocity $V_{c \cdot 0}$ corresponding to $H = 0$. The latter is determined by $R_c = \dfrac{V_{c \cdot 0}}{2\,(a+b)\,\nu}$ giving

(5) $$h_c = \frac{1}{12} \cdot \frac{\eta}{\varrho g} \cdot \frac{V_{c \cdot 0} L}{b a^3} \cdot f^2\,(z_0)$$

where it will be remembered that $f(z_0) = \dfrac{z_0^2 \tanh z_0}{z_0 - \tanh z_0}$ and $z_0 = Ha\sqrt{10^{-9}\varkappa^{-1}\eta^{-1}}$. Equation (5) should represent the boundary curve between the domains of the laminar and the turbulent flow in the case of a flat channel $a \ll b$. In figs. 9—18 the actual boundary curves are drawn in all cases where the observations include the turbulent domain. The boundary curve is of a parabolic character. It is not, of course, to be expected that it can be represented, with all ducts, by the formula (5). In the first instance the product with which $f^2\,(z_0)$ is multiplied will generally not coincide exactly with the ordinate to the boundary curve

3*

for $H = 0$ — owing to shortcomings in the measurement of the dimensions of the ducts. We will therefore direct our attention to the shape of the boundary curve only and we shall make the natural assumption that $f(z_0)$ in (5) must be replaced by $f(c_1 z_0)$ as found in the previous paragraph. That is to say we will assume that, with rectangular ducts, the boundary curve may be represented by

$$(6) \qquad h = h_{0 \cdot B} \cdot \frac{1}{9} \left[f\left(z_0 \cdot 10^{-0.35 \frac{a}{b}}\right) \right]^2 \text{cm. } Hg$$

and with cylindrical pipes by

$$(7) \qquad h = h_{0 \cdot B} \cdot \frac{1}{9} \left[f(0.51 \, z_0) \right]^2 \text{cm. } Hg.$$

These assumptions are put to the test in figs. 9—18 (except fig. 11) where the full drawn curves are the observed curves while the dot-and-dash curves are calculated from (6) or (7). With the cylindrical pipes the agreement between the two curves is perfect so that only the observed curve is drawn. With the rectangular ducts it is still fairly good as long as $a < b$. With $a > b$ larger discrepancies occur, which was of course to be expected.

Appendix I.

Check on the Reynolds' Law of Similarity.

The material of observations of the present research may be utilised for a control of the Reynolds' Law of Similarity in the case of a flow of mercury through cylindrical or rectangular pipes. For from each of the diagrams of which samples are given in figs. 9—18 the variation — at zero field-intensity — of the pressure drop with the

flow, characterised either by the volume-velocity V or by the REYNOLDS' number R, may be derived. We shall here confine ourselves to the observations from cylindrical pipes. Ten years ago the flow of mercury in such pipes was compared to that of water and it was found that the REYNOLDS' Law of Similarity holds good for mercury also[1]. The law was tested in the shape of a curve, having as abscissa the REYNOLDS' number defined by $R_1 = \dfrac{vd}{v}$, d being the internal diameter of the pipe. The ordinate was the quantity $\psi_1 = \dfrac{h}{L\left(\dfrac{4v^2}{gd}\right)}$ where h is the pressure drop in the length L of the pipe. Now it has become customary to define R by $R = \dfrac{vr}{v}$, where r is the radius of the pipe, and to plot the quantity $\psi = \dfrac{h}{L\dfrac{v^2}{gd}} = 4\psi_1$ against R. This we shall do in the following. The earlier test with mercury was performed mainly with wider pipes because it was then found difficult to obtain reproduceable results with narrower pipes. So in all essentials, the test was confined to the part of the $\psi_1 - R_1$ curve corresponding to values of R_1 above 10000. With the new experiments the flow in rather narrow pipes could be studied without any difficulty owing to the introduction of an effective method of cleaning the pipes. The results of these experiments, therefore, supplement the older ones in a very happy way, rendering possible the checking of the law down to very low values of R.

The following pipes were used in the test:

$$K\ 11, \quad d = 0.0689 \text{ cm.}$$
$$K\ 12, \quad d = 0.1165 \text{ cm.}$$

[1] See note p. 3 of Introduction.

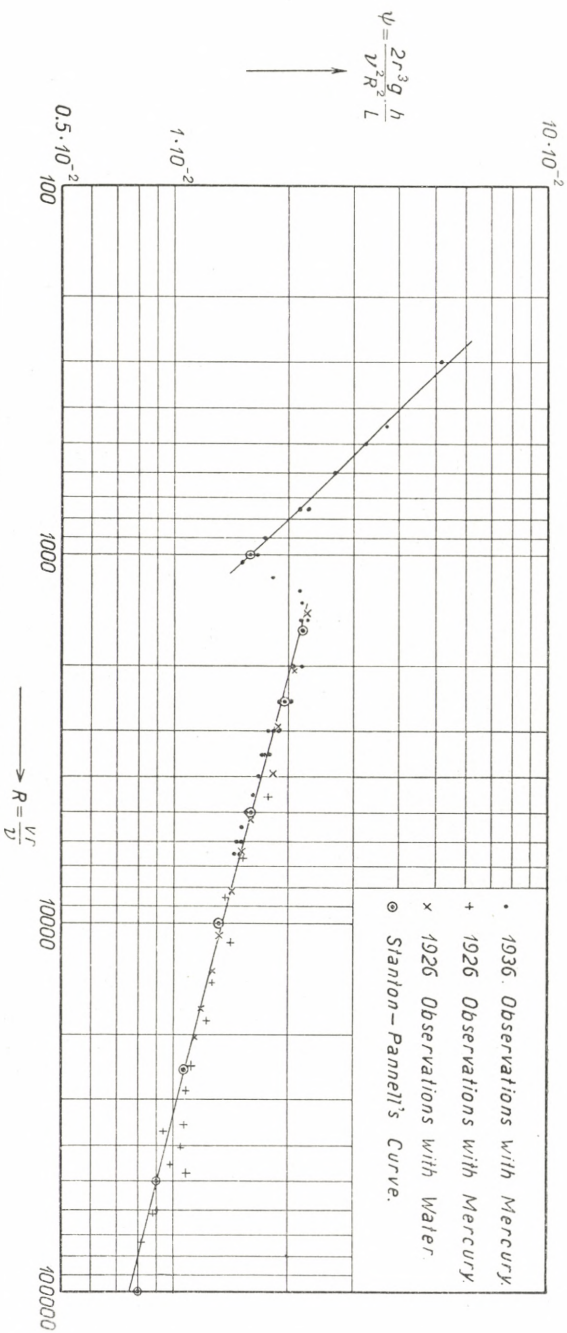Fig. 23. Check on the REYNOLDS' Law of Similarity.

$$\psi = \frac{2r^3 g}{v'^2 R^2} \cdot \frac{h}{L}$$

$$R = \frac{v\Gamma}{\nu}$$

- • 1936. Observations with Mercury.
- + 1926. Observations with Mercury.
- × 1926. Observations with Water.
- ⊚ Stanton—Pannell's Curve.

K 13, $d = 0.1845$ cm.

K 15, $d = 0.3293$ cm.

In all cases the pressure drop was measured over a length of 28 cm. of the pipe. The value of ψ was calculated from the formula:

(1) $$\psi = \frac{2\,r^3 g}{L\,v^2} \cdot \frac{h}{R^2}$$

a form obtained from the formula given above by introducing R instead of v. In Tab. III all the values for ψ are

Tab. III.

$R \cdot 10^{-3}$	$\log_{10} R$	K 11 $\psi \cdot 10^3$	K 12 $\psi \cdot 10^3$	K 13 $\psi \cdot 10^3$	K 15 $\psi \cdot 10^3$
0.30	2.477	51.8	—	—	—
0.45	2.653	35.4	—	—	—
0.50	2.699	—	32.40	—	—
0.60	2.778	26.3	—	—	—
0.75	2.875	21.2	22.48	—	—
0.90	2.954	17.48	—	—	—
1.00	3.000	—	16.68	—	—
1.05	3.021	15.08	—	—	—
1.15	3.061	18.20	—	—	—
1.25	3.097	21.40	19.40	—	—
1.35	3.130	21.75	—	—	—
1.50	3.176	21.30	21.76	21.36	22.24
2.00	3.301	—	20.20	20.12	21.68
2.50	3.398	—	18.92	19.00	20.04
3.00	3.477	—	17.92	18.08	18.76
3.50	3.544	—	17.20	17.40	17.88
4.00	3.602	—	—	16.72	16.76
4.50	3.653	—	—	16.24	16.32
5.00	3 699	—	—	15.68	15.92
5.50	3.740	—	—	15.20	15.40
6.00	3.778	—	—	14.84	15.16
6.50	3.813	—	—	14.56	14.88

stated and in the diagram, fig. 23, they are plotted against R. In the same diagram values of ψ calculated from the

earlier test are entered, and so the $\psi - R$ curve is extended
up to values of R of about 70000, covering nearly the same
interval as the well-known investigations by Stanton and
Pannell[1]. Points from the curve obtained in this latter
investigation are shown in the diagram. Quite obviously
the same law holds good for mercury as for the fluids
examined by Stanton and Pannell. It may be noted that
the curve which may be drawn on the basis of the mer-
cury experiments exhibits the same faint upward bend as
the Stanton-Pannell curve. If this curvature is neglected
and a straight line drawn evenly among the points, the
slope of this line is found to be almost exactly 4, in agree-
ment with the formula given by Blasius. Again, it is
found that the straight line representing the observations
within the laminar domain corresponds, as it should, to
the equation $\psi R = 16$.

Appendix II.

The Influence of the magnetic Field on the turbulent Flow.

From the diagrams figs. 9—18 it is seen that within
the domain of turbulent flow the pressure drop decreases
when the intensity of the magnetic field increases. This of
course is due to a damping of the turbulence, but what is
observed is not the sole effect of this damping. Together
with the smoothing out of the vortices which manifests
itself in a smaller pressure drop there is undoubtedly also
the other effect of the field known from a laminar flow,
thus an effect which tends to increase the pressure drop.
The actual pressure drop is the resultant of these two

[1] Phil. Trans. Royal Soc. A. 214.

effects counteracting each other. In the following the two effects are termed the damping effect and the viscosity effect respectively.

We may make an attempt to isolate the effect of the field on the turbulence i. e. the damping effect. The reasoning on which this attempt is based may be stated as follows. In fig. 24 $h_T b_2 c$ is the observed curve for the variation of the pressure drop in a given length of the tube with a
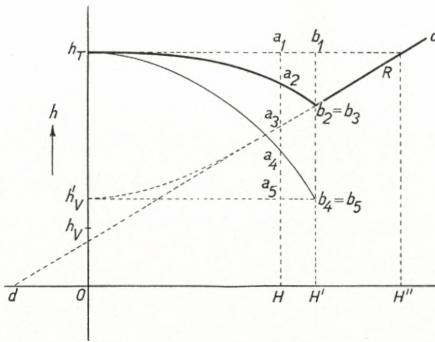

Fig 24. Diagram illustrating attempt at separating the viscosity effect and the damping effect within the domain of turbulent flow.

given flow or a given REYNOLDS' number. Now it would seem very likely that the damping effect i. e. the reduction of the pressure drop due to the damping of the vortices is proportional to the square of the field-intensity. That is to say, it may be anticipated that the curve for the damping effect is a simple parabola. The question then arises: How must the curve for the viscosity effect be in order to make the curve for the damping effect a parabola. Let us assume $h'_V a_3 b_2$ to be the curve for the viscosity effect within the domain of turbulence. Then a point of the curve for the damping effect would be obtained by lowering a corresponding point a_2 of the observed curve

by the amount $a_3 a_5$. In this way the point a_4 is arrived at and the whole curve for the damping effect would be $h_T a_4 b_4$. The problem is to choose $h'_V a_3 b_3$ in such a way that $h_T a_4 b_4$ becomes a parabola. In drawing $h'_V a_3 b_3$ we know one thing for certain, namely that the curve is to pass the point b_3. But in addition we may reasonably make the following assumptions: 1) that the curve in the point b_3 has its tangent in common with the known curve branch $b_3 c$; 2) that the curve has a smooth more or less parabolic shape approximately as indicated; 3) that close to $H = 0$ the tangent is horizontal; and 4) that the curve is higher than the curve corresponding to a laminar flow, i. e. that its ordinate at $H = 0$ is higher than the value of h determined by

$$(1) \qquad\qquad h_V = \frac{8 L \nu^2}{r^3 g} \cdot R.$$

The last assumption requires some explanation. With laminar flow and no field the distribution of velocity across the pipe is parabolic. With turbulent flow, i. e. with the flow which actually obtains in the pipe, the distribution is uniform across most of the diameter, dropping rather abruptly to zero within a zone close to the wall. The latter type of velocity distribution is just that produced by a strong magnetic field acting on a laminar flow and manifesting itself in an increased pressure drop.

This is the reason why we conclude that the curve representing the viscosity effect must at $H = 0$ be drawn through a point h'_V higher than that corresponding to h_V calculated from (1).

The experiments with cylindrical pipes were now dealt with in the way indicated. The most reliable of these experiments with regard to the pressure drop within the
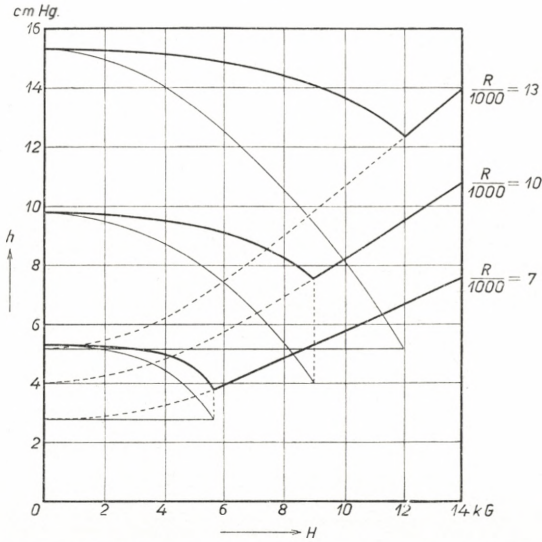
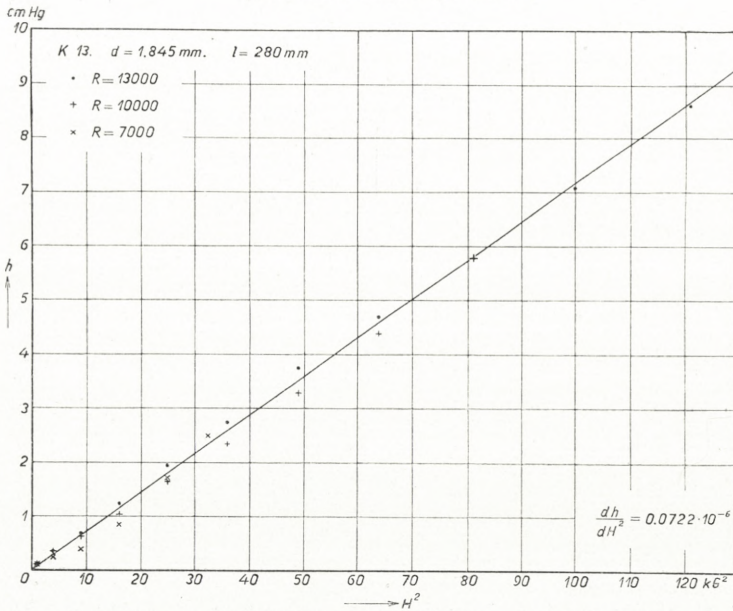Fig. 25. Construction of Curves for the Damping Effect with Experiments performed with Pipe $K13$.

Fig. 26. Test on parabolic Character of the Damping Effect Curve in the Case of Pipe $K13$.

turbulent domain were those performed with the widest pipes: K 13, 14, and 15, while the pressure drop with the narrower pipes K 11 and K 12 was rather uncertain within the said domain due to instability of the flow in the boundary region between the turbulent and the laminar domain. With the pipes K 13, 14, and 15, however, rather characteristic results were arrived at. If the curve $h'_v a_3 b_3$ was drawn in such a way that the ordinate at $H = 0$, h'_v, was twice the height h_v corresponding to a laminar flow $\left(h_v = \dfrac{8 L \nu^2}{r^3 g} R \right)$ then the curve for the damping effect became a parabola and this parabola was found to be independent of the intensity of the flow. In fig. 25 the construction of curves for the damping effect with the pipe K13 is shown and in fig. 26 the test of the parabolic character and of the independency of the intensity of the flow, i. e. of R, is illustrated. From the latter diagrams the values of $\dfrac{dh}{dH^2}$ entered in the following table were found.

Pipe	d cm.	$\dfrac{dh}{dH^2} \cdot 10^6$	$d \cdot \dfrac{dh}{dH^2} \cdot 10^6$
K 12	0.1165	0.0960	0.0112
K 13	0.1845	0.0722	0.0133
K 14	0.2294	0.0571	0.0131
K 15	0.3298	0.0422	0.0139

From the results with K 13, 14, and 15 we tentatively draw the conclusion that the damping effect may be expressed by the simple formula

$$h = 0.0134 \cdot 10^{-6} \frac{H^2}{d} \text{ (Gauss, cm., cm. } Hg)$$

independently of the intensity of the flow (volume-velocity). It should be borne in mind that h is the reduction of the pressure drop due to the damping effect of the field on the

turbulence. It is thus the difference between the ordinates
of the curve for the damping effect at $H = 0$ and at the
field-intensity in question. In the table the values found
with $K\,12$ are also given. They are, however, less reliable.

One may seek a confirmation of the simple relation
for the damping effect by a dimensional consideration. If
it is justifiable to assume that the change in the pressure
drop pr. cm. due to this effect can depend only on 1) the
field intensity H, 2) the diameter d of the pipe, and 3) the
velocity v of the flow then we may write down the equation

$$\frac{h \varrho g}{L} = H^r\,d^s\,v^q.$$

Introducing the dimensions for the various qualities we find
for the determination of r, s and q: $-\frac{r}{2}+s+q = -2,\ \frac{r}{2} = 1,$
$-r-q = -2$ from which $s = -1,\ r = 2,\ q = 0$ and so

$$\frac{h \varrho g}{L} = c_1 \cdot \frac{H^2}{d} \quad \text{(independently of } v,\ V \text{ or } R\text{)}$$

or (with a constant L and with a given liquid)

$$h = c_2 \cdot \frac{H^2}{d}$$

as found above.

It is quite obvious that the attempt at separating the
viscosity effect and the damping effect just explained is to
be considered only as a provisional step in the investigation
of this domain. So too much weight should not be attached
to the results which may on a closer examination prove
more or less false. It is contemplated to make the influence
of the magnetic field on a turbulent flow the subject of a
subsequent investigation.

Provisional Laboratory of Technical Physics. Royal Technical College.
Copenhagen. May 1937.